

The magnetic resonance in high-temperature superconductors: Evidence for an extended s-wave pairing symmetry

Guo-meng Zhao*

Department of Physics and Astronomy, California State University at Los Angeles, Los Angeles, CA 90032, USA

We have identified several important features in the neutron scattering data of cuprates, which are difficult to be explained in terms of d-wave and isotropic s-wave order parameters. Alternatively, we show that the neutron data are in quantitative agreement with an order parameter that has an extended s-wave (A_{1g}) symmetry and opposite sign in the bonding and antibonding electron bands formed within the Cu_2O_4 bilayers. The extended s-wave has eight line nodes and change signs when a node is crossed. This A_{1g} pairing symmetry may be compatible with a charge fluctuation mediated pairing mechanism.

The microscopic pairing mechanism responsible for high-temperature superconductivity in copper-based perovskite oxides is still a subject of intense debate despite tremendous experimental and theoretical efforts for over 15 years. The debate has centered around the role of antiferromagnetic spin fluctuations in high-temperature superconductivity and the symmetry of superconducting condensate (order parameter). Extensive inelastic neutron scattering experiments have accumulated a great deal of important data that should be sufficient to address these central issues. Of particular interest is the magnetic resonance peak that has been observed in double-layer cuprate superconductors such as $\text{YBa}_2\text{Cu}_3\text{O}_y$ (YBCO) [1–6] and $\text{Bi}_2\text{Sr}_2\text{CaCu}_2\text{O}_{8+y}$ (BSCCO) [7,8], and in a single-layer compound $\text{Tl}_2\text{Ba}_2\text{CuO}_{6+y}$ (Tl-2201) [9]. A number of theoretical models [10–13] have been proposed to explain the magnetic resonance peak in terms of d-wave magnetic pairing mechanisms. These theories can qualitatively explain some features of neutron data but are particularly difficult to account for an important feature: The magnetic resonance in optimally and overdoped double-layer cuprates is much more pronounced in the odd channel than in the even channel [2–4]. In order to overcome this difficulty, Mazin and co-worker [14] proposed an order parameter that has isotropic s-wave symmetry and opposite sign in the bonding and antibonding electron bands formed within the Cu_2O_4 bilayers [14]. However, this model predicts that the resonance energy is larger than twice the magnitude of the superconducting gap along the Cu-O bonding direction, in disagreement with experiment. Further, the nodeless s-wave gap symmetry is inconsistent with the measurements of the penetration depth, thermal conductivity and specific heat, which consistently suggest the existence of line nodes in the gap function of hole-doped cuprates [15,16].

Here we identify several important features in the neutron scattering data of cuprates. These features are inconsistent with d-wave order parameter (OP). Alternatively, we show that the neutron data are in quantitative agreement with an order parameter that has an extended s-wave (A_{1g}) symmetry [17,18] and opposite sign in the

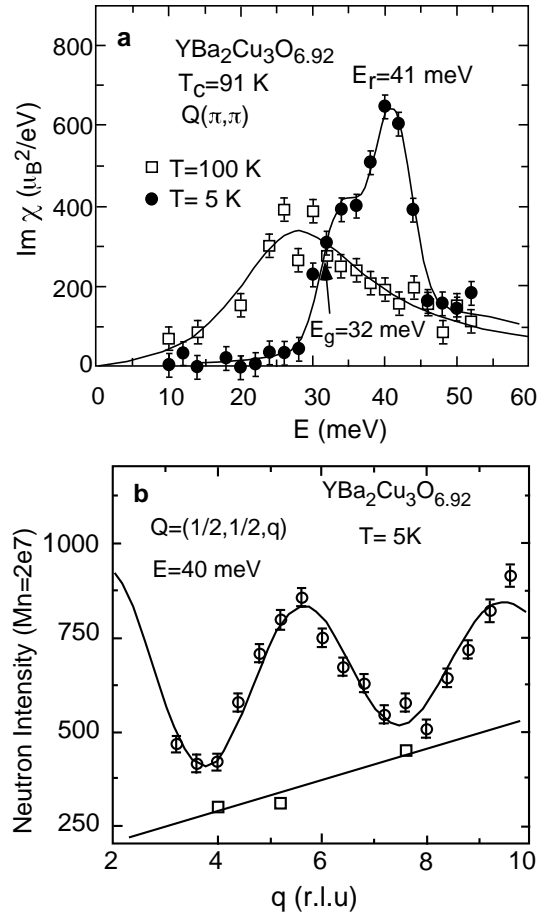


FIG. 1. a) The imaginary part of dynamic spin susceptibility as a function of excitation energy for $\text{YBa}_2\text{Cu}_3\text{O}_{6.92}$ in the normal and superconducting states. The figure was reproduced from Ref. [5]. b) q_i -scan at $E=40$ meV in $\text{YBa}_2\text{Cu}_3\text{O}_{6.92}$ displaying a modulation typical of odd excitation. The figure was reproduced from Ref. [4]. The background (lower line and open squares) was obtained from q -scans across the magnetic line. The upper solid curve is a fit to $a + bF^2(\vec{Q}) \sin^2(\pi z q_i)$, where $F(\vec{Q})$ is the Cu magnetic form factor. The modulation is not complete as even excitations are sizable at $q_i = 3.5, 7$ but with a magnitude 5 times smaller [4].

bonding and antibonding electron bands formed within the Cu_2O_4 bilayers [14].

The magnetic resonance peak observed in optimally doped and overdoped double-layer compounds $\text{YBa}_2\text{Cu}_3\text{O}_y$ [1–5] and $\text{Bi}_2\text{Sr}_2\text{CaCu}_2\text{O}_{8+y}$ [7,8] is a sharp collective mode that occurs at an energy of 38–43 meV and at the two-dimensional wavevector $\vec{Q}_{AF} = (\pi/a, \pi/a)$, where a is the nearest-neighbor Cu-Cu distance. Fig. 1a shows the imaginary part of the odd channel spin susceptibility as a function of excitation energy for a slightly underdoped double-layer compound $\text{YBa}_2\text{Cu}_3\text{O}_{6.92}$. The figure is reproduced from Ref. [5]. There are several striking features in the data: (a) The resonance peak at $E_r = 41$ meV appears below T_c and this resonance peak intensity in the superconducting state $I_{odd}^S(E_r)$ is larger than the normal-state intensity $I_{odd}^N(E_r)$ by a factor of about 3.6, i.e., $I_{odd}^S(E_r)/I_{odd}^N(E_r) = 3.6$; (b) A spin gap feature is seen below T_c and there is a small shoulder that occurs at an energy slightly above the spin gap energy $E_g = 32$ meV. Fig. 1b shows a $q_{||}$ -scan at $E = 40$ meV in $\text{YBa}_2\text{Cu}_3\text{O}_{6.92}$ displaying a modulation typical of odd excitation. The figure is reproduced from Ref. [4]. From Fig. 1b, we find feature (c): The odd-channel magnetic resonance intensity within the Cu_2O_4 bilayers is larger than the even-channel one by a factor of about 5 (Ref. [4]), i.e., $I_{odd}^S(E_r)/I_{even}^S(E_r) = 5$. From the neutron studies on different double-layer compounds with different doping levels, one identifies feature (d): The resonance energy E_r does not increase with doping in the overdoped range but is proportional to T_c as $E_r/k_B T_c \simeq 5.2$ in both underdoped and overdoped ranges [8].

On the other hand, the neutron data for a single-layer Tl-2201 are different from those for double-layer compounds. For the single-layer Tl-2201, we show in Fig. 2a the difference spectrum of the neutron intensities at $T = 27$ K ($< T_c$) and $T = 99$ K ($> T_c$), at a wavevector of $\vec{Q} = (0.5, 0.5, 12.25)$. The figure is reproduced from Ref. [9]. Although a sharp peak feature is clearly seen at $E_r = 46$ meV, it is remarkable that the peak intensity in the superconducting state is close to the magnetic neutron intensity in the normal state, that is, $I^S(E_r)/I^N(E_r) \simeq 1$. This is in sharp contrast with the above result for the double-layer compound $\text{YBa}_2\text{Cu}_3\text{O}_{6.92}$ where we found $I_{odd}^S(E_r)/I_{odd}^N(E_r) = 3.6$. Thus we identify feature (e) as $I^S(E_r)/I^N(E_r) \simeq 1$ for the single-layer compound.

We would like to mention that feature (e) identified for the single-layer Tl-2201 is valid only if the nonmagnetic background has a negligible temperature dependence below 100 K. It is known that nuclear contributions predominantly constitute the main part of the neutron signal [3]. Any nuclear contributions (nonmagnetic backgrounds) are only expected to obey the following standard temperature dependence, $1/[1 - \exp(-E/k_B T)]$ (see detailed discussions in Ref. [3]). In the energy range of interest ($E > 40$ meV), this temperature dependence factor is close to unity and nearly independent of temperature for $T < 150$ K. Indeed, the normal-state neutron intensities of both YBCO [3] and BSCCO [7,8] show a negligible temperature dependence for $T_c < T < 150$ K. For $E =$

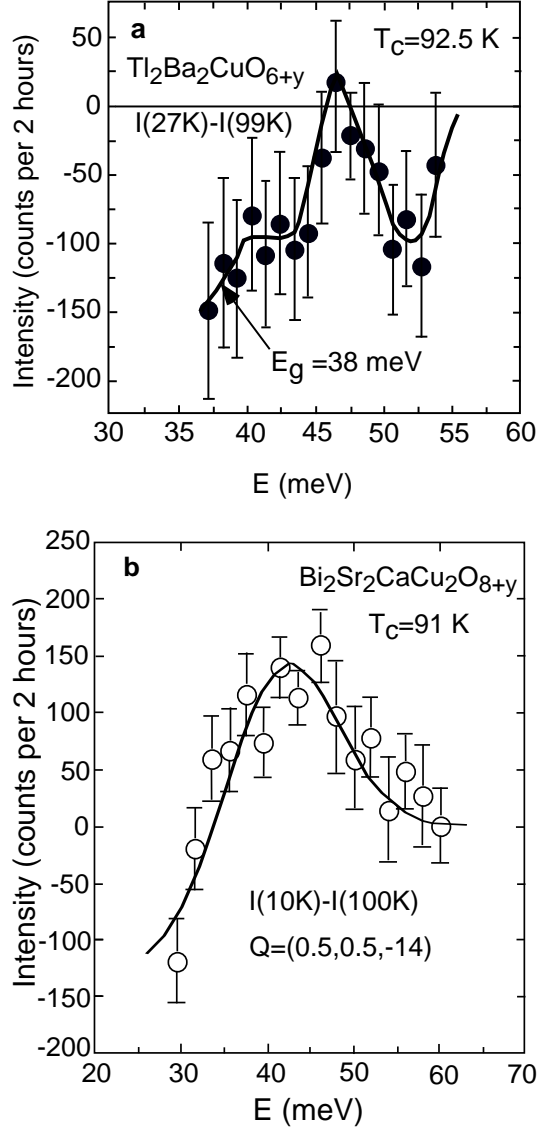


FIG. 2. a) The difference spectrum of the neutron intensities of single-layer Tl-2201 crystals (with a total volume of 0.11 cm^3) at $T = 27$ K ($< T_c$) and $T = 99$ K ($> T_c$), and at wavevector $\vec{Q} = (0.5, 0.5, 12.25)$. The figure is reproduced from Ref. [9]. The solid line is guide to the eye. The difference spectrum tends to zero at about 56 meV (about 10 meV higher than the resonance energy). This suggests that the nonmagnetic background at 56 meV has negligible temperature dependence below 100 K. b) The difference spectrum of the neutron intensities of optimally doped BSCCO crystals (with a total volume of 0.06 cm^3) at $T = 10$ K ($< T_c$) and $T = 100$ K ($> T_c$), and at wavevector $\vec{Q} = (0.5, 0.5, -14)$. The figure is reproduced from Ref. [7]. The difference spectrum goes to zero at 60 meV (about 16 meV higher than the resonance energy). This suggests that the nonmagnetic background at 60 meV has negligible temperature dependence below 100 K.

$E_r = 46$ meV in Tl-2201, the factor $1/[1 - \exp(-E/k_B T)]$ decreases by 0.4% when the temperature is lowered from 99 K to 27 K. If we take the nonmagnetic background of 2500 counts per two hours [9], the nonmagnetic background decreases by 10 counts per two hours when the

temperature goes from 99 K to 27 K, and by 60 counts per two hours when the temperature goes from 150 K to 99 K. The variation of the nonmagnetic background at $E = 46$ meV below 100 K is negligibly small compared with the magnetic resonance intensity (~ 150 counts per two hours). Therefore, feature (e) identified for the single-layer Tl-2201 is well justified.

In order to further justify feature (e), we compare the ratios of the magnetic to the nonmagnetic background signals in those neutron experiments on different compounds. From the neutron data, we find that the signal-to-background ratio is about 6% for Tl-2201 (Ref. [9]), about 12% for an optimally doped BSCCO [7], about 6% for an overdoped BSCCO [8], and about 100% for an overdoped YBCO [3]. The signal-background-ratio in the overdoped BSCCO is similar to that for Tl-2201. But the overdoped BSCCO shows a difference spectrum similar to that for the overdoped YBCO where the signal-background-ratio is larger than that for the overdoped BSCCO by a factor of 20. This suggests that, if feature (e) identified for Tl-2201 were an artifact caused by a small signal-background-ratio, one would not have observed the intrinsic difference spectra for the overdoped BSCCO. The fact that the difference spectra for the overdoped BSCCO are similar to the one for YBCO suggests that one indeed finds the intrinsic magnetic difference spectra for the overdoped BSCCO even though the signal-background-ratio is only 6%. There are no reasons to believe that only the difference spectrum for Tl-2201 is an artifact. Therefore, the pronounced difference between the difference spectrum of the single-layer Tl-2201 and that of the double-layer BSCCO (compare Fig. 2a and Fig. 2b) is due to the fact that $I_{odd}^S(E_r)/I_{odd}^N(E_r) \gg 1$ for the double-layer BSCCO while $I^S(E_r)/I^N(E_r) \sim 1$ for the single-layer Tl-2201. Moreover, we will show below that, for the intraband scattering (even channel) in $\text{YBa}_2\text{Cu}_3\text{O}_{6.92}$, $I_{even}^S(E_r)/I_{even}^N(E_r) = 0.72$, in good agreement with feature (e) for the single-layer Tl-2201. This consistency gives further support to the thesis that feature (e) is intrinsic.

One may also argue that the glue that glues about 300 small crystals of Tl-2201 on Al-plates would cause a substantial decrease of the nonmagnetic background below 100 K. If this argument were relevant, one would have observed a similar effect in overdoped $\text{Y}_{0.9}\text{Ca}_{0.1}\text{Ba}_2\text{Cu}_3\text{O}_{7-y}$ (YBCO-Ca) because 60 larger crystals of YBCO-Ca are also glued on Al-plates [19]. Because the total volume of YBCO-Ca crystals is larger than that of Tl-2201 crystals by a factor of 3.2, one can readily show that the amount of glue for YBCO-Ca crystals is comparable with or even larger than that for Tl-2201. This suggests that the effect of glue on the nonmagnetic background in Tl-2201 is similar to that in YBCO-Ca. From the data for YBCO-Ca (Fig. 2a and Fig. 3a of Ref. [19]), one can clearly see that the difference spectrum at 50 meV is very close to zero. Because the magnetic signal at an energy that is about 10 meV higher than the

resonance energy is independent of temperature below 100 K (see Fig. 1a), the nearly zero value of the difference spectrum at 50 meV implies that the nonmagnetic background at 50 meV has negligible temperature dependence below 100 K in the case of YBCO-Ca. Even in the case of Tl-2201 (see Fig. 2a), the difference spectrum tends to zero at about 56 meV (about 10 meV higher than the resonance energy) although one needs more data points in the vicinity of 56 meV to definitively address this issue. This indicates that the nonmagnetic background at 56 meV has negligible temperature dependence below 100 K in the case of Tl-2201.

We would like to mention that the normal-state magnetic intensities in Fig. 4 of Ref. [9] are significantly underestimated. This is because the authors assume that the q -width of the magnetic peak in the normal state is the same as that in the superconducting state [9]. This assumption is unphysical. From Fig. 19d and Fig. 19h of Ref. [6], one can clearly see that the q -width of the magnetic peak in the normal state is a factor of 1.6 larger than that in the superconducting state in the case of underdoped $\text{YBa}_2\text{Cu}_3\text{O}_{6.8}$. Further, the q -width increases with the increase of doping. With a much broader magnetic peak in the normal state, the q range (0.35 rlu - 0.65 rlu) for the normal-state q -scan spectrum (see Fig. 2B of Ref. [9]) is too narrow to get meaningful estimates of the nonmagnetic background and the normal-state magnetic intensity. Moreover, the normal-state q -scan spectrum of $\text{YBa}_2\text{Cu}_3\text{O}_{6.8}$ is nearly featureless for the same narrow q -range (0.35 rlu - 0.65 rlu), similar to the data of Fig. 2B of Ref. [9]. If one would fit the normal-state q -scan data only in this narrow q -range (0.35 rlu - 0.65 rlu) for $\text{YBa}_2\text{Cu}_3\text{O}_{6.8}$ and assume the same q -width as that in the superconducting state, one would find that the normal-state magnetic intensity is underestimated by a factor of 4. Such a significant underestimate may be also true for the normal-state magnetic intensities of Tl-2201. The authors of Ref. [9] should have extended their measurements to a wider q range to get reliable estimates of the nonmagnetic background and the normal-state magnetic intensities.

Since magnetic signals in both normal and superconducting states strongly depend on doping, as clearly seen in YBCO [4], the comparison of the resonance peak intensities and spectral weights among different compounds should be carefully made. For this Tl-2201, there is some indication of a broad peak centered around \vec{Q}_{AF} even above T_c (Ref. [9]), as observed in underdoped YBCO [4,6]. This suggests that the Tl-2201 is slightly underdoped so that the magnetic intensity in the normal state should be close to that for slightly underdoped $\text{YBa}_2\text{Cu}_3\text{O}_{6.92}$. This is because both compounds have a similar ratio T_c/T_{cm} and thus a similar doping level (where T_{cm} is the superconducting transition at optimal doping). As seen from Fig. 1a, the normal-state magnetic intensity at 40 meV is about $100 \mu_B^2/\text{eV}$ per Cu in slightly underdoped $\text{YBa}_2\text{Cu}_3\text{O}_{6.92}$. The resonance peak

intensity for the Tl-2201 can be estimated to be about $120 \mu_B^2/\text{eV}$ per Cu from the resonance spectral weight of $0.7\mu_B^2$ per Cu (Ref. [9]). Therefore, the resonance peak intensity for the Tl-2201 is close to the normal-state magnetic intensity for the slightly underdoped $\text{YBa}_2\text{Cu}_3\text{O}_{6.92}$. Since the normal-state magnetic intensity for Tl-2201 should be similar to that for the slightly underdoped $\text{YBa}_2\text{Cu}_3\text{O}_{6.92}$, then $I^S(E_r)/I^N(E_r) \simeq 1.2$ for this single-layer Tl-2201. This is in good agreement with feature (e) deduced independently from the difference spectrum (Fig. 2a). Moreover, we find that the resonance peak intensity for the Tl-2201 ($\sim 120 \mu_B^2/\text{eV}$ per Cu) is a factor of about three smaller than the resonance peak intensity for the slightly underdoped $\text{YBa}_2\text{Cu}_3\text{O}_{6.92}$ ($\sim 330 \mu_B^2/\text{eV}$ per Cu). Similarly, the resonance spectral weight for the Tl-2201 is also a factor of three smaller than that for the slightly underdoped $\text{YBa}_2\text{Cu}_3\text{O}_{6.92}$.

These important features we have identified above should place strong constraints on theories for high-temperature superconductivity in cuprates. Any correct theories should be able to explain all the magnetic resonance features in a consistent and quantitative way. In a more exotic approach [10], the neutron data are interpreted in terms of a collective mode in the spin-triplet particle-particle channel, which couples to the particle-hole channel in the superconducting state with d-wave OP. This model predicts that the resonance peak energy E_r is proportional to the doping level p , in disagreement with feature (d): E_r does not increase with increasing p in the overdoped range but is proportional to T_c as $E_r/k_B T_c \simeq 5.2$ (Ref. [8]). Moreover, this model predicts [20] that $E_r > 2\Delta_M$ (where Δ_M is the maximum d-wave gap), which contradicts experiment. Other theories based on spin-fermion interactions also show that E_r increases monotonically with increasing p [11,12], in disagreement with feature (d).

Alternatively, feature (d) is consistent with a simple particle-hole excitation across the superconducting gap within an itinerant magnetism model. This is because the particle-hole excitation energy increases with the superconducting gap which in turn should be proportional to T_c at least in the overdoped range. This itinerant magnetism model is also supported by very recent Fourier transform scanning tunnelling spectroscopic (FT-STs) studies on a nearly optimally doped BSCCO [21], which show that the quasiparticles in the superconducting state exhibit particle-hole mixing similar to that of conventional Fermi-liquid superconductors. These FT-STs results thus provide evidence for a Fermi-liquid behavior in the superconducting state of optimally doped and overdoped cuprates. Here we quantitatively explain all these neutron data [1–9] in terms of an order parameter (OP) that has an extended s-wave symmetry [17,18] and opposite sign in the bonding and antibonding electron bands formed within the Cu_2O_4 bilayers [14]. In our model, the neutron resonance peak is due to excitations of electrons from the extended saddle points below the Fermi level to

the superconducting gap edge above the Fermi level.

Within the itinerant magnetism model, neutron scattering intensity at a wavevector \vec{q} and an energy E is proportional to the imaginary part of the dynamic electron spin susceptibility, $\chi''(\vec{q}, E)$. Qualitatively, with the neglect of the Bardeen-Cooper-Schrieffer (BCS) coherence factor, the bare imaginary part of spin susceptibility, $\chi_c''(\vec{q}, E)$, is proportional to the joint density of states $A(\vec{q}, E) = \sum_{\vec{k}} \delta(E - E_{\vec{k}+\vec{q}} - E_{\vec{k}})$, where $E_{\vec{k}} = \sqrt{\epsilon_{\vec{k}}^2 + \Delta_{\vec{k}}^2}$ is the quasiparticle dispersion law below T_c , $\epsilon_{\vec{k}}$ is the electronic band dispersion, and $\Delta_{\vec{k}}$ is the order parameter [14]. The two particle energy $E_2(\vec{k}, \vec{q}) = E_{\vec{k}+\vec{q}} + E_{\vec{k}}$ has a minimum and several saddle points for a fixed \vec{q} . The minimum defines the threshold energy, or spin gap energy E_g , which is achieved at vector \vec{k} and $\vec{k} + \vec{q}$ such that both \vec{k} and $\vec{k} + \vec{q}$ belong to the Fermi surface and thus $E_g = 2\Delta_{\vec{k}}$ (Ref. [14]).

The joint density of states has divergences at the extended saddle points [14]. The divergent peak in $\chi_c''(\vec{q}, \omega)$ occurs because of transitions between the occupied states located in the extended saddle points below E_F and empty quasiparticle states at the superconducting gap edge above E_F . The saddle points produce Van Hove singularities in the quasiparticle density of states in the superconducting state at an energy of $\sqrt{(\epsilon_{\vec{k}}^{VH})^2 + \Delta_{\vec{k}}^2}$ and the superconducting condensate creates a sharp coherence peak in the quasiparticle density of states at the gap edge. Thus, the divergence in the joint density of states in the superconducting state is then located at the energy $E^* = \Delta_{\vec{k}+\vec{q}} + \sqrt{(\epsilon_{\vec{k}}^{VH})^2 + \Delta_{\vec{k}}^2}$. This simple expression for E^* has been verified by numerical calculations in the case of an isotropic s-wave order parameter [14].

In Fig. 3, we plot the Fermi surface for a slightly underdoped BSCCO, which is inferred by extending a portion of the Fermi surface determined by angle-resolved photoemission spectroscopy (ARPES) [22]. There are extended saddle points that are located near $(\pm\pi, 0)$ and $(0, \pm\pi)$, as shown by ARPES [23]. A solid line in Fig. 3 represents a segment of the extended saddle points very close to the Fermi surface. Other portions of the saddle points [e.g., along the line from $(0, 0)$ to $(\pi, 0)$] are significantly away from the Fermi surface [23] and not shown in the figure. If we only consider the magnetic excitations at a fixed wavevector that corresponds to the antiferromagnetic wavevector \vec{Q}_{AF} , only four electron wavevectors at the Fermi surface are connected by \vec{Q}_{AF} as indicated by arrow 1 in Fig. 3. Each of these vectors forms an angle of θ_r with respect to the Cu-O bonding direction. The electron transitions from the occupied states located at the extended saddle points below E_F to empty quasiparticle states at the superconducting gap edge above E_F are indicated by arrow 2. Because the quasiparticle densities of states at the gap edge and the saddle points are divergent at zero temperature, such transitions will produce a

sharp resonance peak at $E_r = \Delta_{\vec{k}+\vec{Q}_{AF}} + \sqrt{(\epsilon_{\vec{k}}^{VH})^2 + \Delta_{\vec{k}}^2}$ (Ref. [14]).

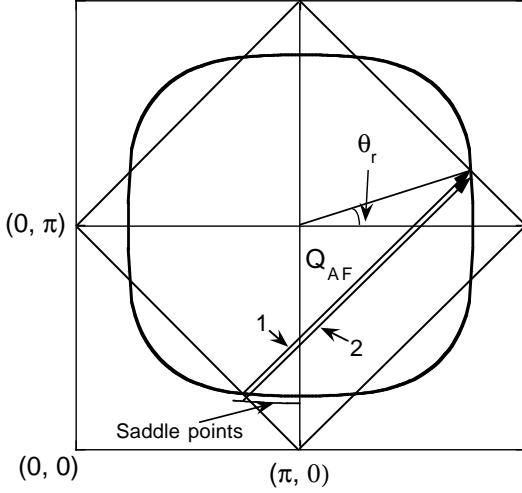


FIG. 3. The Fermi surface for a slightly underdoped BSCCO with $T_c = 88$ K. This Fermi-surface is extrapolated from a part of the Fermi surface determined by ARPES [22] using symmetry arguments. Arrow 1 indicates electron transitions from the occupied states in the superconducting gap edge below E_F to empty quasiparticle states at the gap edge above E_F . Arrow 2 marks electron transitions from the occupied states located in the extended saddle points below E_F to empty quasiparticle states in the superconducting gap edge above E_F .

In terms of θ_r , both $E_g(\vec{Q}_{AF})$ and $E_r(\vec{Q}_{AF})$ can be rewritten as

$$E_g(\vec{Q}_{AF}) = 2\Delta(\theta_r) \quad (1)$$

and

$$E_r(\vec{Q}_{AF}) = \Delta(\theta_r) + \sqrt{[\Delta(\theta_r)]^2 + (\epsilon_r^{VH})^2}. \quad (2)$$

Here $\sqrt{[\Delta(\theta_r)]^2 + (\epsilon_r^{VH})^2}$ is the energy of a saddle point below the Fermi level along the θ_r direction. One should note that Eq. 2 is valid only if the saddle points are very close to the Fermi surface, as is the case.

We now consider the BCS coherence factor that has been ignored in the above discussions. The BCS coherence factor is given by [24]:

$$\xi(\vec{q}, \vec{k}) = \frac{1}{2} \left(1 - \frac{\epsilon_{\vec{k}} \epsilon_{\vec{k}+\vec{q}} + \Delta_{\vec{k}+\vec{q}} \Delta_{\vec{k}}}{E_{\vec{k}} E_{\vec{k}+\vec{q}}} \right). \quad (3)$$

For $\epsilon_{\vec{k}} \ll \Delta_{\vec{k}}$ and $\epsilon_{\vec{k}+\vec{q}} \ll \Delta_{\vec{k}+\vec{q}}$, the BCS coherence factor is close to 1 when $\Delta_{\vec{k}+\vec{q}}$ and $\Delta_{\vec{k}}$ have opposite sign, but is close to zero when $\Delta_{\vec{k}+\vec{q}}$ and $\Delta_{\vec{k}}$ have the same sign. The coherence factor is not negligible for $\epsilon_{\vec{k}} \simeq \Delta_{\vec{k}}$ and $\epsilon_{\vec{k}+\vec{q}} = 0$ even if $\Delta_{\vec{k}+\vec{q}}$ and $\Delta_{\vec{k}}$ have the same sign.

For a single-layer compound with d-wave order parameter symmetry, $\Delta_{\vec{k}+\vec{Q}_{AF}}$ and $\Delta_{\vec{k}}$ have opposite

sign so that the BCS coherence factor $\simeq 1$ and thus $I^S(E_r)/I^N(E_r) \gg 1$ (see Ref. [13]). Therefore, the experimental observation of $I^S(E_r)/I^N(E_r) \sim 1.0$ in the single-layer Tl-2201 [9] rules out the d-wave order parameter. Alternatively, for a single-layer compound with an s-wave symmetry, $\Delta_{\vec{k}+\vec{Q}_{AF}}$ and $\Delta_{\vec{k}}$ have the same sign, so the BCS coherence factor could be much less than 1. This may lead to $I^S(E_r)/I^N(E_r) \sim 1$, in agreement with feature (e). Hence, only the intralayer (intra-band) s-wave symmetry is compatible with feature (e): $I^S(E_r)/I^N(E_r) \sim 1.0$. On the other hand, if extended saddle points are significantly below the Fermi level, the BCS coherence factor will be substantial even for the intralayer (intra-band) magnetic scattering in the case of s-wave gap symmetry. Then $I^S(E_r)/I^N(E_r)$ could be much larger than 1 in this special case. Therefore, the observation of $I^S(E_r)/I^N(E_r) \gg 1$ for the intralayer (intra-band) magnetic scattering is consistent with either s-wave or d-wave gap symmetry.

For a double-layer compound, interactions within Cu_2O_4 bilayers yield bonding and antibonding bands. Transitions between electronic states of the same type (bonding-to-bonding or antibonding-to-antibonding) and those of opposite types are characterized by even or odd symmetry, respectively, under exchange of two adjacent CuO_2 layers. As a result, the magnetic excitations between different bands correspond to odd channel excitations while the excitations within the same band to even channel excitations [4]. If the order parameters in the bonding and antibonding bands have the same sign, the magnetic resonance intensities in both channels should be similar for an intraband pairing symmetry of either s-wave or d-wave. This is because the BCS coherence factors for both channels are the same in this case. On the other hand, if the order parameter has an s-wave symmetry and opposite sign in the bonding and antibonding electron bands, the magnetic resonance intensity in the odd channel will be much larger than that in the even channel due to the large difference in their BCS coherence factors. Therefore, only if the order parameter has an s-wave symmetry and opposite sign in the bonding and antibonding electron bands, can the observed feature (c): $I_{odd}^S(E_r)/I_{even}^S(E_r) = 5$ for the slightly underdoped YBCO and $I_{odd}^S(E_r)/I_{even}^S(E_r) > 10$ for the overdoped YBCO [3] be explained within the itinerant magnetism approach.

Based on the t-J model and d-wave pairing symmetry, Brinckmann and Lee [25] have recently attempted to account for feature (c) using a very unrealistic parameter: $J_{\perp}/J_{\parallel} = 0.6$ (where J_{\parallel} and J_{\perp} are the effective intralayer and interlayer antiferromagnetic exchange energies, respectively). For undoped YBCO, neutron experiments [4] show that $J_{\perp}/J_{\parallel} = 0.1$, which is far less than 0.6 used in the calculation [25]. Further, the value of J_{\perp}/J_{\parallel} will be negligible if J_{\parallel} remains substantial and the optical magnon gap ($\propto \sqrt{J_{\parallel} J_{\perp}}$) goes to zero, which should

be the case for optimally doped and overdoped YBCO. Neutron data for underdoped YBCO [26] show that the optical magnon gap is about 50 meV for $\text{YBa}_2\text{Cu}_3\text{O}_{6.5}$ and is reduced to about 25 meV for $\text{YBa}_2\text{Cu}_3\text{O}_{6.7}$. If we linearly extrapolate the optical magnon gap with the oxygen content, the gap will tend to zero in $\text{YBa}_2\text{Cu}_3\text{O}_y$ for $y > 0.9$, implying that $J_\perp/J_\parallel \ll 0.1$ for optimally doped and overdoped cuprates.

Using a more realistic parameter of J_\perp and the d-wave pairing symmetry, Millis and Monien [27] appear to be able to explain feature (c). They showed that the resonance spectral weights in the odd and even channels are related to the difference between the resonance energy E_r and the particle-hole spin excitation energy $2\Delta(\theta_r)$ at \vec{Q}_{AF} , i.e., $W^{odd}/W^{even} = [2\Delta(\theta_r) - E_r^{odd}]/[2\Delta(\theta_r) - E_r^{even}]$. Here $2\Delta(\theta_r)$ must be larger than both E_r^{even} and E_r^{odd} (Ref. [27]). The INS data of $\text{Y}_{0.9}\text{Ca}_{0.1}\text{Ba}_2\text{Cu}_3\text{O}_{7-y}$ would be consistent with this theoretical model if one would choose an unrealistic parameter $2\Delta(\theta_r) = 49$ meV (Ref. [19]). As discussed below, θ_r is about 15° for slightly overdoped cuprates so that $2\Delta(\theta_r) = 1.73\Delta_M$ (where Δ_M is the maximum d-wave gap). The intrinsic tunneling spectra, which are unsusceptible to surface deterioration, can provide the most reliable determination of the bulk superconducting gap [28]. From the intrinsic tunneling spectra, one finds that $2\Delta_M/k_B T_c = 8.09$ for the optimally doped BSCCO with $T_c = 94$ K (Ref. [28]), $2\Delta_M/k_B T_c = 6.73$ for a slightly overdoped BSCCO with

$T_c = 89$ K (Ref. [28]), and $2\Delta_M/k_B T_c = 5.37$ for an overdoped BSCCO with $T_c = 80$ K (Ref. [29]). It is apparent that $2\Delta_M/k_B T_c$ decreases almost linearly with T_c in the overdoped range. Using the fitted curve of $2\Delta_M/k_B T_c$ versus T_c , we estimate $2\Delta_M/k_B T_c = 6.04$ and $2\Delta(\theta_r) = 38.6$ meV for $\text{Y}_{0.9}\text{Ca}_{0.1}\text{Ba}_2\text{Cu}_3\text{O}_{7-y}$ with $T_c = 85.5$ K. Similarly we can obtain $2\Delta_M/k_B T_c = 5.66$ and $2\Delta(\theta_r) = 35.1$ meV for overdoped BSCCO with $T_c = 83$ K. INS experiment on $\text{Y}_{0.9}\text{Ca}_{0.1}\text{Ba}_2\text{Cu}_3\text{O}_{7-y}$ (Ref. [19]) indicates $E_r^{even} = 43$ meV $> 2\Delta(\theta_r)$, in contradiction with the theoretical model [27]. For overdoped BSCCO with $T_c = 83$ K, $E_r^{odd} = 38$ meV (Ref. [8]) and thus $E_r^{even} = 45$ meV by analogy with the case of $\text{Y}_{0.9}\text{Ca}_{0.1}\text{Ba}_2\text{Cu}_3\text{O}_{7-y}$. Both E_r^{even} and E_r^{odd} in this overdoped BSCCO are far larger than $2\Delta(\theta_r)$, in contradiction with any theoretical models based on the d-wave pairing symmetry.

For the underdoped $\text{YBa}_2\text{Cu}_3\text{O}_{6.7}$, the even-channel magnetic intensity in the normal state is a factor of 2.0-2.5 lower than the odd-channel one for $E = 40$ meV, which is about 15 meV above the optical magnon gap [26]. This implies that the interlayer antiferromagnetic correlation does not influence magnetic excitations well above the optical magnon gap [26]. Since the optical magnon gaps for optimally doped and overdoped YBCO are much smaller than that for the underdoped $\text{YBa}_2\text{Cu}_3\text{O}_{6.7}$, one should expect that $I_{odd}^N(E)/I_{even}^N(E) \simeq 1$ for $E \simeq 40$ meV in optimally doped and overdoped

TABLE I. Comparison of experiments with extended s-wave, d-wave, and isotropic s-wave. In both extended and isotropic s-wave models, the order parameters are assumed to have opposite signs in the bonding and antibonding electron bands formed within the Cu_2O_4 bilayers. Here DA = definitive agreement, A = agreement, QA = qualitative agreement, PA = possible agreement, D = disagreement and DD = definitive disagreement.

INS data	extended s-wave	d-wave	isotropic s-wave
Feature (a): $I^S(E_r)/I^N(E_r) = 3.6$ for YBCO	DA	DA	DA
Feature (c): $I_{odd}^S(E_r)/I_{even}^S(E_r) = 5$ for YBCO	DA	DD	DA
Feature (e): $I^S(E_r)/I^N(E_r) < 1$ for Tl-2201	DA	DD	DA
The magnitudes of E_r and E_g	DA	DD	DD
Spin gap in $\text{La}_{2-x}\text{Sr}_x\text{CuO}_4$	DA	DD	DD
Other data	extended s-wave	d-wave	isotropic s-wave
Penetration depth	DA	QA	DD
Thermal conductivity	DA	QA	DD
Specific heat	DA	QA	DD
Nonlinear Meissner effect	DA	QA	DD
ARPES (underdoped)	A	A	DD
ARPES (overdoped)	DA	DD	DD
Quasiparticle tunneling (underdoped)	PA	PA	DD
Quasiparticle tunneling (overdoped)	DA	DD	DD
Raman scattering (underdoped)	PA	PA	DD
Raman scattering (overdoped)	DA	DD	PA
NMR/NQR	A	A	DD
Andreev reflection	A	PA	DD
Pb/c-axis YBCO Josephson junction	A	D	A
c-axis BSCCO twist Josephson junction	DA	DD	PA
Corner SQUID/Josephson junction	PA	PA	PA
Tricrystal/Tetracrystal Josephson junctions	PA	PA	PA

YBCO. Thus the observed feature (c): $I_{odd}^S(E_r)/I_{even}^S(E_r) \gg 1$ for optimally doped and overdoped YBCO can only be explained by an OP that has s-wave symmetry and opposite sign in the bonding and antibonding electron bands.

For the slightly underdoped $\text{YBa}_2\text{Cu}_3\text{O}_{6.92}$, we can also deduce the value of $I_{even}^S(E_r)/I_{even}^N(E_r)$ using the measured $I_{odd}^S(E_r)/I_{odd}^N(E_r) = 3.6$, $I_{odd}^S(E_r)/I_{even}^S(E_r) = 5$, and the inferred $I_{odd}^N(E_r)/I_{even}^N(E_r) \simeq 1$ (see above discussion). From the measured $I_{odd}^S(E_r)/I_{even}^S(E_r) = 5$, we have $I_{even}^S(E_r) = 0.2I_{odd}^S(E_r)$ and thus $I_{even}^S(E_r)/I_{even}^N(E_r) \simeq 0.2I_{odd}^S(E_r)/I_{odd}^N(E_r) = 0.72$. This value is close to that deduced for the single-layer Tl-2201 ($\simeq 1$). These results consistently suggest that the intraband neutron intensity at E_r in the superconducting state is close to that in the normal state. This unique and important feature we have identified rules out d-wave order parameter symmetry because d-wave symmetry predicts [13,25] that $I_{even}^S(E_r)/I_{even}^N(E_r) \gg 1$ for bilayer compounds and $I^S(E_r)/I^N(E_r) \gg 1$ for single-layer compounds.

From Eqs. 1 and 2, it is easy to calculate E_g and E_r if one knows the gap function $\Delta(\theta)$ and the θ_r value. From the measured Fermi surface, one can readily determine θ_r . For example, we find $\theta_r = 18.4^\circ$ for a slightly underdoped BSCCO from Fig. 3. For optimally doped cuprates, we get $\theta_r \simeq 16.0^\circ$. If we would use an isotropic s-wave gap function $\Delta(\theta) = 28$ meV for a slightly overdoped YBCO, we would have $E_g = 56$ meV and $E_r > 56$ meV, which are far larger than the measured $E_g = 33$ meV and $E_r = 40$ meV (Ref. [3]). If we would use a d-wave gap function $\Delta(\theta) = 28\cos 2\theta$ meV, we would have $E_g = 47.5$ meV and $E_r > 47.5$ meV, which are also far larger than the measured values. Thus, one cannot quantitatively explain the neutron data in terms of d-wave and isotropic s-wave symmetries.

Alternatively, an extended s-wave with eight line nodes (A_{1g} symmetry) is in quantitative agreement with two-thirds of the experiments that were designed to test the order-parameter symmetry for hole-doped cuprates [17]. The remaining one-third (e.g., tricrystal grain-boundary Josephson junction experiments) are explained qualitatively by Zhao [17] and by Brandow [18]. In Table 1, we compare nearly all the experiments used to test the OP symmetry with the extended s-wave, d-wave, and isotropic s-wave models. In both extended s-wave and isotropic s-wave models, the order parameters are assumed to have opposite sign in the bonding and antibonding electron bands formed within the Cu_2O_4 bilayers [14]. The detailed comparisons with other experiments are made in Ref. [17]. From Table 1, one can see that the neutron data alone provide a definitive answer to the intrinsic, bulk OP symmetry because INS is a bulk, phase and angle sensitive technique. Other bulk and non-phase sensitive experiments provide complementary support to the present conclusions. The phase and surface sensitive experiments cannot definitively determine the intrinsic

bulk OP symmetry because the surface OP might be different from the bulk one [17].

For a slightly overdoped YBCO, more than six independent experiments consistently suggest that [17] the gap function is $\Delta(\theta) = 24.5(\cos 4\theta + 0.225)$ meV. Substituting $\theta_r = 16^\circ$ into the gap function, we get $\Delta(\theta_r) = 16.3$ meV and thus $E_g = 32.6$ meV, in quantitative agreement with the measured one (32-33 meV).

In our model, the position of the extended saddle point along the θ_r direction is located at $E_r - E_g/2$ in the superconducting state (see Eqs. 1 and 2). For optimally doped YBCO with $E_r = 41$ meV and $E_g = 32$ meV, we find that the saddle point in the superconducting state is located at an energy of 25 meV below the Fermi level. This is in agreement with the ARPES studies [30] which suggest that the Fermi level in the superconducting state for optimally doped cuprates is ≤ 30 meV above the extended saddle points that have the same energy over a large momentum space [23]. Further, electronic Raman scattering spectra in $\text{YBa}_2\text{Cu}_4\text{O}_8$ have been used to determine the energy of the extended saddle points more accurately [31]. At 10 K (well below T_c), the energy of the extended saddle points is found to be 24.3 meV below the Fermi level, in excellent agreement with the result predicted by our model from the INS data ($\simeq 25$ meV).

We have identified the unique and important feature: $I^S(E_r)/I^N(E_r) \simeq 1.0$ for the intralayer and intraband magnetic scattering. This feature unambiguously rules out the d-wave OP symmetry. The unambiguous determination of the intrinsic extended s-wave pairing symmetry for hole-doped cuprates places strong constraints on the pairing mechanism for high-temperature superconductivity. A recent calculation suggests that high energy Cu-O charge fluctuations can lead to an attractive interaction between conduction electrons and the pairing symmetry may be of extended s-wave (A_{1g}) [32].

Indeed, precise thermal-difference reflectance spectra of several cuprate superconductors ($T_c = 105\text{-}120$ K) exhibit pronounced features at photon energies of about 2.0 eV, which may be related to the Cu-O charge fluctuations (Ref. [33]). These features can be well described within Eliashberg theory with an electron-boson coupling constant λ_{ch} of about 0.40. In order to explain a superconducting transition temperature of 105-120 K, the authors simulated [33] an electron-phonon coupling feature at 50 meV with the coupling constant λ_{ph} of about 1.0. This Eliashberg model's simulated electron-phonon coupling agrees well with the results obtained from first principle calculations [34].

The contribution of this 2 eV component can be equivalent to a *negative* Coulomb pseudopotential μ^* within Eliashberg theory [35]. By using a realistic electron-phonon coupling spectral weight deduced from tunneling spectra and a $\mu^* = -0.15$, and taking into a polaronic effect, Zhao *et al.* [35] are able to explain the negligible isotope effect on T_c , and the magnitudes of T_c and the superconducting gap for optimally doped 90 K supercon-

ductors.

In summary, we have identified several important features in the neutron scattering data of cuprates, which are difficult to be explained in terms of d-wave and isotropic s-wave order parameters. Alternatively, we show that the neutron data are in quantitative agreement with an order parameter that has an extended s-wave (A_{1g}) symmetry and opposite sign in the bonding and antibonding electron bands formed within the Cu_2O_4 bilayers. This A_{1g} pairing symmetry may be compatible with a charge fluctuation mediated pairing mechanism. High-temperature superconductivity in cuprates may be due to the combination of strong electron-phonon coupling and substantial electron-charge-fluctuation coupling [33,35].

*Correspondence should be addressed to gzhao2@calstatela.edu

-
- [1] P. Bourges, Y. Sidis, B. Hennion, R. Villeneuve, G. Collin, and J. F. Marucco, *Physica B*, **213-214**, 48 (1995).
- [2] H. F. Fong, B. Keimer, P. W. Anderson, D. Reznik, F. Dogan, and I. A. Aksay, *Phys. Rev. Lett.* **75**, 316 (1995).
- [3] P. Bourges, L. P. Regnault, Y. Sidis, and C. Vettier, *Phys. Rev. B* **53**, 876 (1996).
- [4] P. Bourges, *The gap Symmetry and Fluctuations in High Temperature Superconductors*, Edited by J. Bok, G. Deutscher, D. Pavuna, and S. A. Wolf. S. A. (Plenum Press, 1998) p 349 (Vol. 371 in NATO ASI series, Physics).
- [5] P. Bourges, Y. Sidis, H. F. Fong, B. Keimer, L. P. Regnault, J. Bossy, A. S. Ivanov, D. L. Milius, and I. A. Aksay, *High Temperature Superconductivity*, Edited by Barnes S. E. *et al* p207 (CP483 American Institute of Physics, Amsterdam, 1999)
- [6] P. C. Dai, H. A. Mook, R. D. Hunt, and F. Dogan, *Phys. Rev. B* **63**, 054525 (2001).
- [7] H. F. Fong, P. Bourges, Y. Sidis, L. P. Regnault, A. Ivanov, G. D. Guk, N. Koshizuka, and B. Keimer, *Nature(London)* **398**, 588 (1999).
- [8] H. He, Y. Sidis, P. Bourges, G. D. Gu, A. Ivanov, N. Koshizuka, B. Liang, C. T. Lin, L. P. Regnault, E. Schoenherr, and B. Keimer, *Phys. Rev. Lett.* **86**, 1610 (2001)
- [9] H. He, P. Bourges, Y. Sidis, C. Ulrich, L. P. Regnault, S. Pailhes, N. S. Berzigiarova, N. N. Kolesnikov, and B. Keimer, *Science* **295**, 1045 (2002).
- [10] E. Demler and S. C. Zhang, *Phys. Rev. Lett.* **75**, 4126 (1995).
- [11] A. Abanov and A. V. Chubukov, *Phys. Rev. Lett.* **83**, 1652 (1999).
- [12] D. K. Morr and D. Pines, *Phys. Rev. Lett.* **81**, 1086 (1998).
- [13] J. Brinckmann and P. A. Lee, *Phys. Rev. Lett.* **82**, 2915 (1999).
- [14] I. I. Mazin and V. M. Yakovenko, *Phys. Rev. Lett.* **75**, 4134 (1995).
- [15] W. N. Hardy, D. A. Bonn, D. C. Morgan, Ruixing Liang, and K. Zhang, *Phys. Rev. Lett.* **70**, 3999 (1993).
- [16] M. Chiao, R. W. Hill, C. Lupien, L. Taillefer, P. Lambert, R. Gagnon, and P. Fournier, *Phys. Rev. B* **62**, 3554 (2000).
- [17] G. M. Zhao, *Phys. Rev. B* **64**, 024503 (2001).
- [18] B. H. Brandow, *Phys. Rev. B* **65**, 054503 (2002).
- [19] S. Pailhes, Y. Sidis, P. Bourges, C. Ulrich, V. Hinkov, L.P. Regnault, A. Ivanov, B. Liang, C.T. Lin, C. Bernhard, and B. Keimer, cond-mat/0308394.
- [20] O. Tchernyshyov, M. R. Norman, and A. V. Chubukov, *Phys. Rev. B* **63**, 144507 (2001).
- [21] K. McElroy, R. W. Simmonds, J. E. Hoffman, D.-H. Lee, J. Orenstein, H. Eisaki, S. Uchida, and J. C. Davis, *J. C. Nature (London)* **422**, 592 (2003).
- [22] P. J. White, Z.-X. Shen, C. Kim, J. M. Harris, A. G. Loeser, P. Fournier, and A. Kapitulnik, *Phys. Rev. B* **54**, R15 669 (1996).
- [23] D. S. Dessau, Z.-X. Shen, D. M. King, D. S. Marshall, L. W. Lombardo, P. H. Dickinson, A. G. Loeser, J. DiCarlo, C.-H. Park, A. Kapitulnik, and W. E. Spicer, *Phys. Rev. Lett.* **71**, 2781 (1993).
- [24] J. R. Schrieffer, *Theory of Superconductivity*, (Frontiers in Physics (20), Addison Wesley, 1988).
- [25] J. Brinckmann and P. Lee, *Phys. Rev. B* **65**, 014502 (2001).
- [26] H. F. Fong, P. Bourges, Y. Sidis, L. P. Regnault, J. Bossy, A. Ivanov, D. L. Milius, I. A. Aksay, and B. Keimer, *Phys. Rev. B* **61**, 14773 (2000).
- [27] A. J. Millis and H. Monien, *Phys. Rev. B* **54**, 16172 (1996).
- [28] V.M. Krasnov, A. Yurgens, D. Winkler, P. Delsing, and T. Claeson, *Phys. Rev. Lett.* **84**, 5860 (2000).
- [29] A. Yurgens, D.Winkler, T.Claeson, S. J. Hwang, J. H. Choy, *Int. J. Mod. Phys. B* **13**, 3758 (1999).
- [30] D. M. King, Z.-X. Shen, D. S. Dessau, D. S. Marshall, C. H. Park, W. E. Spicer, J. L. Peng, Z. Y. Li, and R. L. Greene, *Phys. Rev. Lett.* **73**, 3298 (1994).
- [31] E. Ya. Sherman and O. V. Misochko, *Phys. Rev. B* **59**, 195 (1999).
- [32] M. Gulacsi and R. J. Chan, *J. Supercond.* **14**, 651 (2001), and private communication with M. Gulacsi.
- [33] M. J. Holcomb, J. P. Collman, and W. A. Little, *Phys. Rev. Lett.* **73**, 2360 (1994); M. J. Holcomb, C. L. Perry, J. P. Collman, and W. A. Little, *Phys. Rev. B* **53**, 6734 (1996); M. J. Holcomb, *Phys. Rev. B* **54**, 6648 (1996).
- [34] W. E. Pickett, *Rev. Mod. Phys.* **61**, 434 (1989).
- [35] G. M. Zhao, V. Kirtikar, and D. E. Morris, *Phys. Rev. B* **63**, R220506 (2001).